PHYSICAL REVIEW D **82,** 051101(R) (2010)

Study of $B \to X\gamma$ decays and determination of $|V_{td}/V_{ts}|$

P. del Amo Sanchez,[1] J. P. Lees,[1] V. Poireau,[1] E. Prencipe,[1] V. Tisserand,[1] J. Garra Tico,[2] E. Grauges,[2] M. Martinelli,[3a,3b] A. Palano,[3a,3b] M. Pappagallo,[3a,3b] G. Eigen,[4] B. Stugu,[4] L. Sun,[4] M. Battaglia,[5] D. N. Brown,[5] B. Hooberman,[5] L. T. Kerth,[5] Yu. G. Kolomensky,[5] G. Lynch,[5] I. L. Osipenkov,[5] T. Tanabe,[5] C. M. Hawkes,[6] A. T. Watson,[6] H. Koch,[7] T. Schroeder,[7] D. J. Asgeirsson,[8] C. Hearty,[8] T. S. Mattison,[8] J. A. McKenna,[8] A. Khan,[9] A. Randle-Conde,[9] V. E. Blinov,[10] A. R. Buzykaev,[10] V. P. Druzhinin,[10] V. B. Golubev,[10] A. P. Onuchin,[10] S. I. Serednyakov,[10] Yu. I. Skovpen,[10] E. P. Solodov,[10] K. Yu. Todyshev,[10] A. N. Yushkov,[10] M. Bondioli,[11] S. Curry,[11] D. Kirkby,[11] A. J. Lankford,[11] M. Mandelkern,[11] E. C. Martin,[11] D. P. Stoker,[11] H. Atmacan,[12] J. W. Gary,[12] F. Liu,[12] O. Long,[12] G. M. Vitug,[12] C. Campagnari,[13] T. M. Hong,[13] D. Kovalskyi,[13] J. D. Richman,[13] A. M. Eisner,[14] C. A. Heusch,[14] J. Kroseberg,[14] W. S. Lockman,[14] A. J. Martinez,[14] T. Schalk,[14] B. A. Schumm,[14] A. Seiden,[14] L. O. Winstrom,[14] C. H. Cheng,[15] D. A. Doll,[15] B. Echenard,[15] D. G. Hitlin,[15] P. Ongmongkolkul,[15] F. C. Porter,[15] A. Y. Rakitin,[15] R. Andreassen,[16] M. S. Dubrovin,[16] G. Mancinelli,[16] B. T. Meadows,[16] M. D. Sokoloff,[16] P. C. Bloom,[17] W. T. Ford,[17] A. Gaz,[17] J. F. Hirschauer,[17] M. Nagel,[17] U. Nauenberg,[17] J. G. Smith,[17] S. R. Wagner,[17] R. Ayad,[18,*] W. H. Toki,[18] T. M. Karbach,[19] J. Merkel,[19] A. Petzold,[19] B. Spaan,[19] K. Wacker,[19] M. J. Kobel,[20] K. R. Schubert,[20] R. Schwierz,[20] D. Bernard,[21] M. Verderi,[21] P. J. Clark,[22] S. Playfer,[22] J. E. Watson,[22] M. Andreotti,[23a,23b] D. Bettoni,[23a] C. Bozzi,[23a] R. Calabrese,[23a,23b] A. Cecchi,[23a,23b] G. Cibinetto,[23a,23b] E. Fioravanti,[23a,23b] P. Franchini,[23a,23b] E. Luppi,[23a,23b] M. Munerato,[23a,23b] M. Negrini,[23a,23b] A. Petrella,[23a,23b] L. Piemontese,[23a] R. Baldini-Ferroli,[24] A. Calcaterra,[24] R. de Sangro,[24] G. Finocchiaro,[24] M. Nicolaci,[24] S. Pacetti,[24] P. Patteri,[24] I. M. Peruzzi,[24,†] M. Piccolo,[24] M. Rama,[24] A. Zallo,[24] R. Contri,[25a,25b] E. Guido,[25a,25b] M. Lo Vetere,[25a,25b] M. R. Monge,[25a,25b] S. Passaggio,[25a] C. Patrignani,[25a,25b] E. Robutti,[25a] S. Tosi,[25a,25b] B. Bhuyan,[26] C. L. Lee,[27] M. Morii,[27] A. Adametz,[28] J. Marks,[28] S. Schenk,[28] U. Uwer,[28] F. U. Bernlochner,[29] M. Ebert,[29] H. M. Lacker,[29] T. Lueck,[29] A. Volk,[29] P. D. Dauncey,[30] M. Tibbetts,[30] P. K. Behera,[31] U. Mallik,[31] C. Chen,[32] J. Cochran,[32] H. B. Crawley,[32] L. Dong,[32] W. T. Meyer,[32] S. Prell,[32] E. I. Rosenberg,[32] A. E. Rubin,[32] Y. Y. Gao,[33] A. V. Gritsan,[33] Z. J. Guo,[33] N. Arnaud,[34] M. Davier,[34] D. Derkach,[34] J. Firmino da Costa,[34] G. Grosdidier,[34] F. Le Diberder,[34] A. M. Lutz,[34] B. Malaescu,[34] A. Perez,[34] P. Roudeau,[34] M. H. Schune,[34] J. Serrano,[34] V. Sordini,[34,‡] A. Stocchi,[34] L. Wang,[34] G. Wormser,[34] D. J. Lange,[35] D. M. Wright,[35] I. Bingham,[36] J. P. Burke,[36] C. A. Chavez,[36] J. P. Coleman,[36] J. R. Fry,[36] E. Gabathuler,[36] R. Gamet,[36] D. E. Hutchcroft,[36] D. J. Payne,[36] C. Touramanis,[36] A. J. Bevan,[37] F. Di Lodovico,[37] R. Sacco,[37] M. Sigamani,[37] G. Cowan,[38] S. Paramesvaran,[38] A. C. Wren,[38] D. N. Brown,[39] C. L. Davis,[39] A. G. Denig,[40] M. Fritsch,[40] W. Gradl,[40] A. Hafner,[40] K. E. Alwyn,[41] D. Bailey,[41] R. J. Barlow,[41] G. Jackson,[41] G. D. Lafferty,[41] T. J. West,[41] J. Anderson,[42] R. Cenci,[42] A. Jawahery,[42] D. A. Roberts,[42] G. Simi,[42] J. M. Tuggle,[42] C. Dallapiccola,[43] E. Salvati,[43] R. Cowan,[44] D. Dujmic,[44] P. H. Fisher,[44] G. Sciolla,[44] M. Zhao,[44] D. Lindemann,[45] P. M. Patel,[45] S. H. Robertson,[45] M. Schram,[45] P. Biassoni,[46a,46b] A. Lazzaro,[46a,46b] V. Lombardo,[46a] F. Palombo,[46a,46b] S. Stracka,[46a,46b] L. Cremaldi,[47] R. Godang,[47,§] R. Kroeger,[47] P. Sonnek,[47] D. J. Summers,[47] X. Nguyen,[48] M. Simard,[48] P. Taras,[48] G. De Nardo,[49a,49b] D. Monorchio,[49a,49b] G. Onorato,[49a,49b] C. Sciacca,[49a,49b] G. Raven,[50] H. L. Snoek,[50] C. P. Jessop,[51] K. J. Knoepfel,[51] J. M. LoSecco,[51] W. F. Wang,[51] L. A. Corwin,[52] K. Honscheid,[52] R. Kass,[52] J. P. Morris,[52] A. M. Rahimi,[52] N. L. Blount,[53] J. Brau,[53] R. Frey,[53] O. Igonkina,[53] J. A. Kolb,[53] R. Rahmat,[53] N. B. Sinev,[53] D. Strom,[53] J. Strube,[53] E. Torrence,[53] G. Castelli,[54a,54b] E. Feltresi,[54a,54b] N. Gagliardi,[54a,54b] M. Margoni,[54a,54b] M. Morandin,[54a] M. Posocco,[54a] M. Rotondo,[54a] F. Simonetto,[54a,54b] R. Stroili,[54a,54b] E. Ben-Haim,[55] G. R. Bonneaud,[55] H. Briand,[55] G. Calderini,[55] J. Chauveau,[55] O. Hamon,[55] Ph. Leruste,[55] G. Marchiori,[55] J. Ocariz,[55] J. Prendki,[55] S. Sitt,[55] M. Biasini,[56a,56b] E. Manoni,[56a,56b] C. Angelini,[57a,57b] G. Batignani,[57a,57b] S. Bettarini,[57a,57b] M. Carpinelli,[57a,57b,‖] G. Casarosa,[57a,57b] A. Cervelli,[57a,57b] F. Forti,[57a,57b] M. A. Giorgi,[57a,57b] A. Lusiani,[57a,57c] N. Neri,[57a,57b] E. Paoloni,[57a,57b] G. Rizzo,[57a,57b] J. J. Walsh,[57a] D. Lopes Pegna,[58] C. Lu,[58] J. Olsen,[58] A. J. S. Smith,[58] A. V. Telnov,[58] F. Anulli,[59a] E. Baracchini,[59a,59b] G. Cavoto,[59a] R. Faccini,[59a,59b] F. Ferrarotto,[59a] F. Ferroni,[59a,59b] M. Gaspero,[59a,59b] L. Li Gioi,[59a] M. A. Mazzoni,[59a] G. Piredda,[59a] F. Renga,[59a,59b] T. Hartmann,[60] T. Leddig,[60] H. Schröder,[60] R. Waldi,[60] T. Adye,[61] B. Franek,[61] E. O. Olaiya,[61] F. F. Wilson,[61] S. Emery,[62] G. Hamel de Monchenault,[62] G. Vasseur,[62] Ch. Yèche,[62] M. Zito,[62] M. T. Allen,[63] D. Aston,[63] D. J. Bard,[63] R. Bartoldus,[63] J. F. Benitez,[63] C. Cartaro,[63] M. R. Convery,[63] J. Dorfan,[63] G. P. Dubois-Felsmann,[63] W. Dunwoodie,[63] R. C. Field,[63] M. Franco Sevilla,[63] B. G. Fulsom,[63] A. M. Gabareen,[63] M. T. Graham,[63] P. Grenier,[63] C. Hast,[63] W. R. Innes,[63] M. H. Kelsey,[63] H. Kim,[63] P. Kim,[63] M. L. Kocian,[63] D. W. G. S. Leith,[63] S. Li,[63] B. Lindquist,[63] S. Luitz,[63] V. Luth,[63] H. L. Lynch,[63] D. B. MacFarlane,[63] H. Marsiske,[63] D. R. Muller,[63] H. Neal,[63] S. Nelson,[63] C. P. O'Grady,[63] I. Ofte,[63] M. Perl,[63] T. Pulliam,[63] B. N. Ratcliff,[63] A. Roodman,[63] A. A. Salnikov,[63] V. Santoro,[63]

R. H. Schindler,[63] J. Schwiening,[63] A. Snyder,[63] D. Su,[63] M. K. Sullivan,[63] S. Sun,[63] K. Suzuki,[63] J. M. Thompson,[63] J. Va'vra,[63] A. P. Wagner,[63] M. Weaver,[63] C. A. West,[63] W. J. Wisniewski,[63] M. Wittgen,[63] D. H. Wright,[63] H. W. Wulsin,[63] A. K. Yarritu,[63] C. C. Young,[63] V. Ziegler,[63] X. R. Chen,[64] W. Park,[64] M. V. Purohit,[64] R. M. White,[64] J. R. Wilson,[64] S. J. Sekula,[65] M. Bellis,[66] P. R. Burchat,[66] A. J. Edwards,[66] T. S. Miyashita,[66] S. Ahmed,[67] M. S. Alam,[67] J. A. Ernst,[67] B. Pan,[67] M. A. Saeed,[67] S. B. Zain,[67] N. Guttman,[68] A. Soffer,[68] P. Lund,[69] S. M. Spanier,[69] R. Eckmann,[70] J. L. Ritchie,[70] A. M. Ruland,[70] C. J. Schilling,[70] R. F. Schwitters,[70] B. C. Wray,[70] J. M. Izen,[71] X. C. Lou,[71] F. Bianchi,[72a,72b] D. Gamba,[72a,72b] M. Pelliccioni,[72a,72b] M. Bomben,[73a,73b] L. Lanceri,[73a,73b] L. Vitale,[73a,73b] N. Lopez-March,[74] F. Martinez-Vidal,[74] D. A. Milanes,[74] A. Oyanguren,[74] J. Albert,[75] Sw. Banerjee,[75] H. H. F. Choi,[75] K. Hamano,[75] G. J. King,[75] R. Kowalewski,[75] M. J. Lewczuk,[75] I. M. Nugent,[75] J. M. Roney,[75] R. J. Sobie,[75] T. J. Gershon,[76] P. F. Harrison,[76] J. Ilic,[76] T. E. Latham,[76] E. M. T. Puccio,[76] H. R. Band,[77] X. Chen,[77] S. Dasu,[77] K. T. Flood,[77] Y. Pan,[77] R. Prepost,[77] C. O. Vuosalo,[77] and S. L. Wu[77]

(*BABAR* Collaboration)

[1]*Laboratoire d'Annecy-le-Vieux de Physique des Particules (LAPP), Université de Savoie, CNRS/IN2P3, F-74941 Annecy-Le-Vieux, France*
[2]*Universitat de Barcelona, Facultat de Fisica, Departament ECM, E-08028 Barcelona, Spain*
[3a]*INFN Sezione di Bari, I-70126 Bari, Italy*
[3b]*Dipartimento di Fisica, Università di Bari, I-70126 Bari, Italy*
[4]*University of Bergen, Institute of Physics, N-5007 Bergen, Norway*
[5]*Lawrence Berkeley National Laboratory and University of California, Berkeley, California 94720, USA*
[6]*University of Birmingham, Birmingham, B15 2TT, United Kingdom*
[7]*Ruhr Universität Bochum, Institut für Experimentalphysik 1, D-44780 Bochum, Germany*
[8]*University of British Columbia, Vancouver, British Columbia, Canada V6T 1Z1*
[9]*Brunel University, Uxbridge, Middlesex UB8 3PH, United Kingdom*
[10]*Budker Institute of Nuclear Physics, Novosibirsk 630090, Russia*
[11]*University of California at Irvine, Irvine, California 92697, USA*
[12]*University of California at Riverside, Riverside, California 92521, USA*
[13]*University of California at Santa Barbara, Santa Barbara, California 93106, USA*
[14]*University of California at Santa Cruz, Institute for Particle Physics, Santa Cruz, California 95064, USA*
[15]*California Institute of Technology, Pasadena, California 91125, USA*
[16]*University of Cincinnati, Cincinnati, Ohio 45221, USA*
[17]*University of Colorado, Boulder, Colorado 80309, USA*
[18]*Colorado State University, Fort Collins, Colorado 80523, USA*
[19]*Technische Universität Dortmund, Fakultät Physik, D-44221 Dortmund, Germany*
[20]*Technische Universität Dresden, Institut für Kern- und Teilchenphysik, D-01062 Dresden, Germany*
[21]*Laboratoire Leprince-Ringuet, CNRS/IN2P3, Ecole Polytechnique, F-91128 Palaiseau, France*
[22]*University of Edinburgh, Edinburgh EH9 3JZ, United Kingdom*
[23a]*INFN Sezione di Ferrara, I-44100 Ferrara, Italy*
[23b]*Dipartimento di Fisica, Università di Ferrara, I-44100 Ferrara, Italy*
[24]*INFN Laboratori Nazionali di Frascati, I-00044 Frascati, Italy*
[25a]*INFN Sezione di Genova, I-16146 Genova, Italy*
[25b]*Dipartimento di Fisica, Università di Genova, I-16146 Genova, Italy*
[26]*Indian Institute of Technology Guwahati, Guwahati, Assam, 781 039, India*
[27]*Harvard University, Cambridge, Massachusetts 02138, USA*
[28]*Universität Heidelberg, Physikalisches Institut, Philosophenweg 12, D-69120 Heidelberg, Germany*
[29]*Humboldt-Universität zu Berlin, Institut für Physik, Newtonstr. 15, D-12489 Berlin, Germany*
[30]*Imperial College London, London, SW7 2AZ, United Kingdom*
[31]*University of Iowa, Iowa City, Iowa 52242, USA*
[32]*Iowa State University, Ames, Iowa 50011-3160, USA*
[33]*Johns Hopkins University, Baltimore, Maryland 21218, USA*
[34]*Laboratoire de l'Accélérateur Linéaire, IN2P3/CNRS et Université Paris-Sud 11, Centre Scientifique d'Orsay, B. P. 34, F-91898 Orsay Cedex, France*
[35]*Lawrence Livermore National Laboratory, Livermore, California 94550, USA*
[36]*University of Liverpool, Liverpool L69 7ZE, United Kingdom*
[37]*Queen Mary, University of London, London, E1 4NS, United Kingdom*
[38]*University of London, Royal Holloway and Bedford New College, Egham, Surrey TW20 0EX, United Kingdom*
[39]*University of Louisville, Louisville, Kentucky 40292, USA*

[40]*Johannes Gutenberg-Universität Mainz, Institut für Kernphysik, D-55099 Mainz, Germany*
[41]*University of Manchester, Manchester M13 9PL, United Kingdom*
[42]*University of Maryland, College Park, Maryland 20742, USA*
[43]*University of Massachusetts, Amherst, Massachusetts 01003, USA*
[44]*Massachusetts Institute of Technology, Laboratory for Nuclear Science, Cambridge, Massachusetts 02139, USA*
[45]*McGill University, Montréal, Québec, Canada H3A 2T8*
[46a]*INFN Sezione di Milano, I-20133 Milano, Italy*
[46b]*Dipartimento di Fisica, Università di Milano, I-20133 Milano, Italy*
[47]*University of Mississippi, University, Mississippi 38677, USA*
[48]*Université de Montréal, Physique des Particules, Montréal, Québec, Canada H3C 3J7*
[49a]*INFN Sezione di Napoli, I-80126 Napoli, Italy*
[49b]*Dipartimento di Scienze Fisiche, Università di Napoli Federico II, I-80126 Napoli, Italy*
[50]*NIKHEF, National Institute for Nuclear Physics and High Energy Physics, NL-1009 DB Amsterdam, The Netherlands*
[51]*University of Notre Dame, Notre Dame, Indiana 46556, USA*
[52]*Ohio State University, Columbus, Ohio 43210, USA*
[53]*University of Oregon, Eugene, Oregon 97403, USA*
[54a]*INFN Sezione di Padova, I-35131 Padova, Italy*
[54b]*Dipartimento di Fisica, Università di Padova, I-35131 Padova, Italy*
[55]*Laboratoire de Physique Nucléaire et de Hautes Energies, IN2P3/CNRS, Université Pierre et Marie Curie-Paris6, Université Denis Diderot-Paris7, F-75252 Paris, France*
[56a]*INFN Sezione di Perugia, I-06100 Perugia, Italy*
[56b]*Dipartimento di Fisica, Università di Perugia, I-06100 Perugia, Italy*
[57a]*INFN Sezione di Pisa, I-56127 Pisa, Italy*
[57b]*Dipartimento di Fisica, Università di Pisa, I-56127 Pisa, Italy*
[57c]*Scuola Normale Superiore di Pisa, I-56127 Pisa, Italy*
[58]*Princeton University, Princeton, New Jersey 08544, USA*
[59a]*INFN Sezione di Roma, I-00185 Roma, Italy*
[59b]*Dipartimento di Fisica, Università di Roma La Sapienza, I-00185 Roma, Italy*
[60]*Universität Rostock, D-18051 Rostock, Germany*
[61]*Rutherford Appleton Laboratory, Chilton, Didcot, Oxon, OX11 0QX, United Kingdom*
[62]*CEA, Irfu, SPP, Centre de Saclay, F-91191 Gif-sur-Yvette, France*
[63]*SLAC National Accelerator Laboratory, Stanford, California 94309 USA*
[64]*University of South Carolina, Columbia, South Carolina 29208, USA*
[65]*Southern Methodist University, Dallas, Texas 75275, USA*
[66]*Stanford University, Stanford, California 94305-4060, USA*
[67]*State University of New York, Albany, New York 12222, USA*
[68]*Tel Aviv University, School of Physics and Astronomy, Tel Aviv, 69978, Israel*
[69]*University of Tennessee, Knoxville, Tennessee 37996, USA*
[70]*University of Texas at Austin, Austin, Texas 78712, USA*
[71]*University of Texas at Dallas, Richardson, Texas 75083, USA*
[72a]*INFN Sezione di Torino, I-10125 Torino, Italy*
[72b]*Dipartimento di Fisica Sperimentale, Università di Torino, I-10125 Torino, Italy*
[73a]*INFN Sezione di Trieste, I-34127 Trieste, Italy*
[73b]*Dipartimento di Fisica, Università di Trieste, I-34127 Trieste, Italy*
[74]*IFIC, Universitat de Valencia-CSIC, E-46071 Valencia, Spain*
[75]*University of Victoria, Victoria, British Columbia, Canada V8W 3P6*
[76]*Department of Physics, University of Warwick, Coventry CV4 7AL, United Kingdom*
[77]*University of Wisconsin, Madison, Wisconsin 53706, USA*
(Received 21 May 2010; published 10 September 2010)

Using a sample of 471×10^6 $B\bar{B}$ events collected with the *BABAR* detector, we study the sum of seven exclusive final states $B \to X_{s(d)}\gamma$, where $X_{s(d)}$ is a strange (nonstrange) hadronic system with a mass of up to 2.0 GeV/c^2. After correcting for unobserved decay modes, we obtain a branching fraction for $b \to d\gamma$

*Now at Temple University, Philadelphia, Pennsylvania 19122, USA.
†Also with Università di Perugia, Dipartimento di Fisica, Perugia, Italy.
‡Also with Università di Roma La Sapienza, I-00185 Roma, Italy.
§Now at University of South Alabama, Mobile, Alabama 36688, USA.
‖Also with Università di Sassari, Sassari, Italy.

of $(9.2 \pm 2.0(\text{stat}) \pm 2.3(\text{syst})) \times 10^{-6}$ in this mass range, and a branching fraction for $b \to s\gamma$ of $(23.0 \pm 0.8(\text{stat}) \pm 3.0(\text{syst})) \times 10^{-5}$ in the same mass range. We find $\frac{\mathcal{B}(b\to d\gamma)}{\mathcal{B}(b\to s\gamma)} = 0.040 \pm 0.009(\text{stat}) \pm 0.010(\text{syst})$, from which we determine $|V_{td}/V_{ts}| = 0.199 \pm 0.022(\text{stat}) \pm 0.024(\text{syst}) \pm 0.002(\text{th})$.

DOI: 10.1103/PhysRevD.82.051101 PACS numbers: 14.40.Nd, 12.15.Hh

The decays $b \to d\gamma$ and $b \to s\gamma$ are flavor-changing neutral current processes forbidden at tree level in the standard model (SM). The leading-order processes are one-loop electroweak penguin diagrams, for which the top quark is the dominant virtual particle. In theories beyond the SM, new virtual particles may appear in the loop, which could lead to measurable effects on experimental observables such as branching fractions and CP asymmetries [1]. In the SM the inclusive rate for $b \to d\gamma$ is suppressed relative to $b \to s\gamma$ by a factor $|V_{td}/V_{ts}|^2$, where V_{td} and V_{ts} are Cabibbo-Kobayashi-Maskawa matrix elements. Measurements of $|V_{td}/V_{ts}|$ using the exclusive modes $B \to (\rho, \omega)\gamma$ and $B \to K^*\gamma$ [2,3] are now well established, with theoretical uncertainties of 7% from weak annihilation and hadronic form factors [4]. This ratio can also be obtained from the B_d and B_s mixing frequencies and is found to be $0.206 \pm 0.0007(\text{exp}) + 0.0081 - 0.0060(\text{th})$ [5]. It is important to confirm the consistency of the two methods of determining $|V_{td}/V_{ts}|$, since new physics effects would enter in different ways in mixing and radiative decays. A measurement of the branching fractions of inclusive $b \to d\gamma$ relative to $b \to s\gamma$ would determine $|V_{td}/V_{ts}|$ with reduced theoretical uncertainties compared to that from exclusive modes [6].

This paper supersedes [7], and presents the first significant observation of the $b \to d\gamma$ transition in the hadronic mass range $M(X_d) > 1.0\ \text{GeV}/c^2$, resulting in a significant improvement in the determination of $|V_{td}/V_{ts}|$ via the ratio of inclusive widths. Inclusive $b \to s\gamma$ and $b \to d\gamma$ rates are extrapolated from the measurements of the partial decay rates to seven exclusive final states (see Table I) in the hadronic mass ranges $0.5 < M(X_d) < 1.0\ \text{GeV}/c^2$ (low mass, containing the previously measured K^*, ρ and ω resonances) and $1.0 < M(X_d) < 2.0\ \text{GeV}/c^2$ (high mass). We combine these measurements and make a model-dependent extrapolation to higher hadronic mass to obtain an inclusive branching fraction ($\mathcal{B}$) for $b \to (s, d)\gamma$. These measurements use the full data set of $471 \times 10^6\ B\bar{B}$ pairs collected at the $\Upsilon(4S)$ resonance at the PEP-II B factory with the *BABAR* detector [8].

High-energy photons are reconstructed from an isolated energy cluster in the barrel of the calorimeter, with shape consistent with a single photon, and energy $1.15 < E^*_\gamma < 3.50$ GeV, where * denotes the center-of-mass (CM) frame of the $B\bar{B}$ system. We remove photons that can form a π^0 (η) candidate in association with another photon of energy greater than 30 (250) MeV if the two-photon invariant mass is in the range $110 < m_{\gamma\gamma} < 160$ $(520 < m_{\gamma\gamma} < 560)\ \text{MeV}/c^2$ for the low mass region and $95 < m_{\gamma\gamma} < 155$ $(530 < m_{\gamma\gamma} < 565)\ \text{MeV}/c^2$ for the high mass region.

Charged pion and kaon candidates are selected from well-reconstructed tracks. We use a pion selection algorithm to differentiate pions from kaons, with a typical selection efficiency of 95% and kaon misidentification rate of 4%. Kaons are identified as tracks failing the pion selection criteria. We reconstruct $\pi^0(\eta)$ candidates from pairs of photons of minimum energy 20 MeV with an invariant mass $115 < m_{\gamma\gamma} < 150$ $(470 < m_{\gamma\gamma} < 620)\ \text{MeV}/c^2$. We require all pion, eta, and kaon candidates to have a momentum in the laboratory frame greater than 600 (425) MeV/c in the low (high) mass region.

The selected pion, eta, kaon, and high-energy photon candidates are combined to form B meson candidates consistent with one of the seven decay modes. The charged particles are combined to form a common vertex, whose χ^2 probability is required to be greater than 1%. We use the kinematic variables $\Delta E = E^*_B - E^*_{\text{beam}}$, where E^*_B is the energy of the B meson candidate and E^*_{beam} is the beam energy, and $m_{\text{ES}} = \sqrt{E^{*2}_{\text{beam}} - \vec{p}^{\,*2}_B}$, where $\vec{p}^{\,*}_B$ is the momentum of the B candidate. We consider candidates in the range $-0.3 < \Delta E < 0.2$ GeV and $m_{\text{ES}} > 5.22\ \text{GeV}/c^2$.

Contributions from continuum processes ($e^+e^- \to q\bar{q}$, with $q = u, d, s, c$) are reduced by considering only events for which the ratio R_2 of second-to-zeroth order Fox-Wolfram moments [9] is less than 0.98. To further discriminate between the jetlike continuum background and the more spherically symmetric signal events, we compute the angle θ^*_T between the photon momentum and the thrust axis of the rest of the event (ROE) and require $|\cos(\theta^*_T)| < 0.8$. The ROE is defined as all charged tracks and neutral energy deposits that are not used to reconstruct the B candidate.

Ten other event shape variables that distinguish between signal and continuum events are combined in a neural

TABLE I. The reconstructed decay modes. Charge conjugate states are implied throughout this paper.

$B \to X_d\gamma$	$B \to X_s\gamma$
$B^0 \to \pi^+\pi^-\gamma$	$B^0 \to K^+\pi^-\gamma$
$B^+ \to \pi^+\pi^0\gamma$	$B^+ \to K^+\pi^0\gamma$
$B^+ \to \pi^+\pi^-\pi^+\gamma$	$B^+ \to K^+\pi^+\pi^-\gamma$
$B^0 \to \pi^+\pi^-\pi^0\gamma$	$B^0 \to K^+\pi^-\pi^0\gamma$
$B^0 \to \pi^+\pi^-\pi^+\pi^-\gamma$	$B^0 \to K^+\pi^-\pi^+\pi^-\gamma$
$B^+ \to \pi^+\pi^-\pi^+\pi^0\gamma$	$B^+ \to K^+\pi^-\pi^+\pi^0\gamma$
$B^+ \to \pi^+\eta\gamma$	$B^+ \to K^+\eta\gamma$

network (NN). These include the ratio R_2', which is R_2 calculated in the frame recoiling against the photon momentum; the B meson production angle with respect to the beam axis in the CM frame; θ_B^*; and the L-moments [10] of the ROE with respect to either the thrust axis of the ROE or the direction of the high-energy photon. Differences in lepton, pion, and kaon production between background and B decays are exploited by including several flavor-tagging variables applied to the ROE [11]. Using the NN output, we reject 99% of continuum background while preserving 25% of signal decays.

After all selections are applied, there remain events with more than one B candidate. In these events the candidate with the reconstructed π^0 or η mass closest to nominal is retained. Where there is no π^0 or η we retain the candidate with the highest vertex χ^2 probability.

The signal yields in the data for the sum of the seven decay modes are determined from two-dimensional extended maximum likelihood fits to the ΔE and $m_{\rm ES}$ distributions. We consider the following contributions: signal, combinatorial backgrounds from continuum processes, backgrounds from other B decays, and cross-feed from misreconstructed $B \to X\gamma$ decays. The fits to $B \to X_d\gamma$ events contain components from misidentified $b \to s\gamma$ decays, with an expected contribution of 345 events. We neglect the small $b \to d\gamma$ background in the fits to $B \to X_s\gamma$ events.

Each contribution is modeled by a probability density function (PDF) that is determined from Monte Carlo (MC) simulated events unless otherwise specified. For the misidentified signal cross-feed components, we use a binned two-dimensional PDF to account for correlations. All the other PDFs are products of one-dimensional functions of ΔE and $m_{\rm ES}$. For signal, the $m_{\rm ES}$ spectrum is described by a Crystal Ball function [12], and ΔE by a Cruijff function [13]. The parameters of these functions are determined from the fit to the high-statistics $B \to X_s\gamma$ data sample. We use these fitted values to fix the signal shape in the fits to $B \to X_d\gamma$ events.

The remaining B backgrounds contain a small component that peaks in $m_{\rm ES}$ but not ΔE, which is modeled by a Gaussian distribution in $m_{\rm ES}$. Continuum and other non-peaking backgrounds are described by an ARGUS shape [14] in $m_{\rm ES}$ and a second-order polynomial in ΔE.

We perform separate fits for $B \to X_d\gamma$ and $B \to X_s\gamma$ in each of the hadronic mass ranges 0.5–1.0 GeV$/c^2$ and 1.0–2.0 GeV$/c^2$. For each of the four fits, we combine the component PDFs and fit for the signal, generic B and continuum yields, the ARGUS and two polynomial shape parameters. We scale the cross-feed contributions proportionally to the fitted signal yield, refit and iterate until the procedure converges. Projections of $m_{\rm ES}$ and ΔE from fits to data for $B \to X_s\gamma$ and $B \to X_d\gamma$ are shown in the low mass region in Fig. 1 and in the high mass region in Fig. 2. Table II gives the signal yields, efficiencies (after correc-

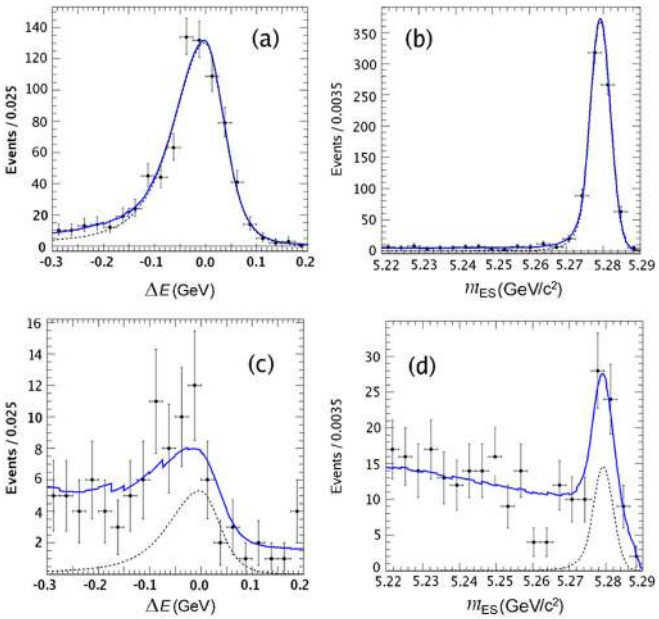

FIG. 1 (color online). Projections of ΔE with $5.275 < m_{\rm ES} < 5.286$ GeV$/c^2$ for (a) $B \to X_s\gamma$ and (c) $B \to X_d\gamma$, and of $m_{\rm ES}$ with $-0.1 < \Delta E < 0.05$ GeV for (b) $B \to X_s\gamma$ and (d) $B \to X_d\gamma$ in the mass range 0.5–1.0 GeV$/c^2$. Data points are compared with the sum of all the fit contributions (solid line). The jagged line is an artifact of the fit projection over the sum of several binned histograms. The dashed line shows the signal component.

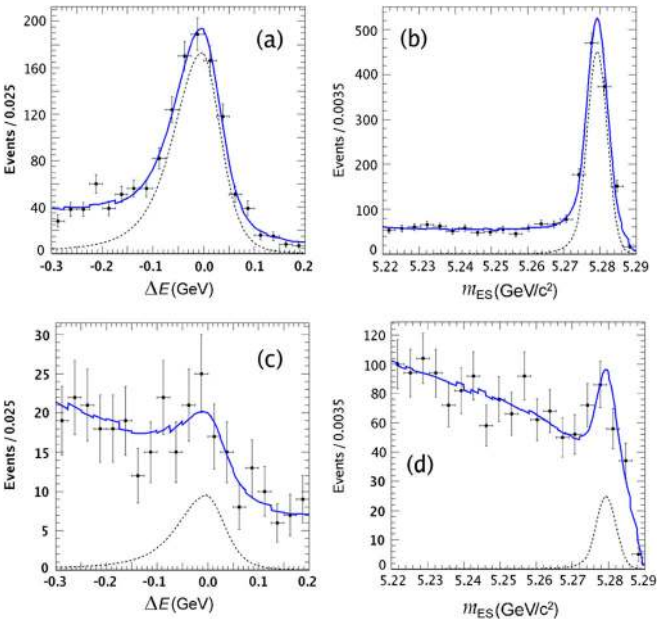

FIG. 2 (color online). Projections of ΔE with $5.275 < m_{\rm ES} < 5.286$ GeV$/c^2$ for (a) $B \to X_s\gamma$ and (c) $B \to X_d\gamma$, and of $m_{\rm ES}$ with $-0.1 < \Delta E < 0.05$ GeV for (b) $B \to X_s\gamma$ and (d) $B \to X_d\gamma$ in the mass range 1.0–2.0 GeV$/c^2$. Data points are compared with the sum of all the fit contributions (solid line). The jagged line is an artifact of the fit projection over the sum of several binned histograms. The dashed line shows the signal component.

TABLE II. Signal yields (N_S), efficiencies (ϵ), partial branching fractions ($\mathcal{PB}$), inclusive branching fractions ($\mathcal{B}$) and the ratio of inclusive branching fractions for the measured decay modes. The first error is statistical and second is systematic (including an error from extrapolation to missing decay modes, for the inclusive $\mathcal{B}$).

	$M(X_s)0.5$–1.0	$M(X_d)0.5$–1.0	$M(X_s)1.0$–2.0	$M(X_d)1.0$–2.0	$M(X_s)0.5$–2.0	$M(X_d)0.5$–2.0
N_S	804 ± 33	35 ± 9	990 ± 42	56 ± 14	...	...
ϵ	4.5%	3.1%	1.6%	1.9%	...	...
$\mathcal{PB}(\times 10^{-6})$	$19 \pm 1 \pm 1$	$1.2 \pm 0.3 \pm 0.1$	$66 \pm 3 \pm 6$	$3.2 \pm 0.8 \pm 0.5$	...	...
$\mathcal{B}(\times 10^{-6})$	$38 \pm 2 \pm 2$	$1.3 \pm 0.3 \pm 0.1$	$192 \pm 8 \pm 29$	$7.9 \pm 2.0 \pm 2.2$	$230 \pm 8 \pm 30$	$9.2 \pm 2.0 \pm 2.3$
$\frac{\mathcal{B}(b\to d\gamma)}{\mathcal{B}(b\to s\gamma)}$	$0.033 \pm 0.009 \pm 0.003$		...	...	$0.040 \pm 0.009 \pm 0.010$	

tions for systematic effects) and partial branching fractions ($\mathcal{PB}$). We calculate $\mathcal{PB}$ using $\mathcal{PB}(B \to X\gamma) = N_S/(2\epsilon N_{B\bar{B}})$, where $N_{B\bar{B}}$ is the number of $B\bar{B}$ pairs in the data sample.

We have investigated a number of sources of systematic uncertainty in the measurement of the partial branching fractions, some of which are common to both $B \to X_d\gamma$ and $B \to X_s\gamma$ and cancel in the ratio of branching fractions (see Table III: those that do not cancel in the ratio are marked by an asterisk). Uncertainties in tracking efficiency, particle identification, γ and π^0 reconstruction, and the π^0/η veto have been evaluated using independent control samples of data and MC simulated events, and incorporated into our analysis. Uncertainty due to the NN selection has been evaluated by comparing the efficiency of the selection in data and MC for the $B \to X_s\gamma$ events, which are relatively free of background, assuming that potential discrepancies between data and MC are the same for the $B \to X_d\gamma$ sample. The means and widths of the signal PDF are varied within the range allowed by the fit to the $B \to X_s\gamma$ data, accounting for correlations. Other PDF parameters are also varied within the 1σ limits determined from the fit to MC. We vary the $b \to s\gamma$ background in the fit to $B \to X_d\gamma$ by the statistical uncertainty on our measurement of those decays. The signal cross feed originating from our measured channels is varied by the statistical uncertainty on our measurement; other signal cross-feed backgrounds by $\pm 50\%$. An additional uncertainty on the efficiency arises from the fragmentation of the hadronic system among the measured final states. For $B \to X_s\gamma$ the uncertainty is constrained by the errors on the measured data; for $B \to X_d\gamma$ an estimate is obtained from the difference between the default phase-space fragmentation (see below) and a reweighting using the measured data/MC differences in $B \to X_s\gamma$.

To obtain inclusive $\mathcal{B}(b \to s\gamma)$ and $\mathcal{B}(b \to d\gamma)$ we need to correct the partial $\mathcal{B}$ values in Table II for the fractions of missing final states. After correcting for the 50% of

TABLE III. Systematic errors on the measured partial and inclusive branching fractions $\mathcal{B}$. Systematic errors that do not cancel in the ratio of rates are marked with (*).

Systematic	$M(X_s)$		$M(X_d)$	
Error source	0.5–1.0	1.0–2.0	0.5–1.0	1.0–2.0
Track selection	0.3%	0.4%	0.3%	0.4%
Photon reconstruction	1.8%	1.8%	1.8%	1.8%
π^0/η reconstruction	0.9%	1.1%	1.4%	1.6%
Neural network	1.1%	4.9%	1.1%	4.9%
B counting	0.6%	0.6%	0.6%	0.6%
PID (*)	2.0%	2.0%	2.0%	2.0%
Fit bias (*)	0.1%	0.9%	4.9%	6.5%
PDF shapes (*)	2.3%	0.6%	3.7%	3.4%
Histogram binning (*)	0.8%	0.2%	1.8%	1.8%
Background (*)	0.8%	1.2%	5.9%	7.0%
Fragmentation (*)	...	3.3%	...	5.1%
Signal model	...	5.8%	...	6.0%
Error on partial $\mathcal{B}$	4.0%	9.0%	9.3%	14.2%
Missing ≥ 5 body		9.6%		18.2%
Other missing states		7.5%		15.3%
Spectrum model		1.8%		1.6%
Error on inclusive $\mathcal{B}$	4.0%	15.2%	9.3%	27.7%

missing decay modes with neutral kaons, the low mass $B \to X_s\gamma$ measurement is found to be consistent with previous measurements of the rate for $B \to K^*\gamma$ [15]. For the low mass $B \to X_d\gamma$ region, we correct for the small amount of nonreconstructed ω final states (for example, $\omega \to \pi^0\gamma$), and find a partial branching fraction consistent with previous measurements of $\mathcal{B}(B \to (\rho, \omega)\gamma)$ [15]. We assume that nonresonant decays do not contribute in this region.

In the high mass region, the missing fractions depend on the fragmentation of the hadronic system and are expected to be different for X_d and X_s. In our signal MC, fragmentation is modeled by selecting an array of final-state particles and resonances according to the phase-space probability of the final state, as implemented by JETSET [16]. We further constrain the distribution of X_s final states to that observed for our seven decay modes as well as the distributions of a number of other states measured in [17]. According to this MC model we reconstruct 43% of the total width in $b \to d\gamma$ and 36% in $b \to s\gamma$. A further 37% of the width of $b \to s\gamma$ is constrained by the isospin relation between charged and neutral kaon decays. We explore the uncertainty in the correction for missing modes by considering several alternative models: replacing 50% of $b \to s\gamma$ and $b \to d\gamma$ hadronic final states with a mix of resonances; varying $b \to s\gamma$ fragmentation constraints within their statistical uncertainties; and setting the $b \to d\gamma$ fragmentation rates to those of their corresponding $b \to s\gamma$ states. The resulting missing fractions vary by up to 50(40)% relative to the nominal model in $B \to X_s\gamma$ ($B \to X_d\gamma$). We therefore independently vary final states with ≥ 5 stable hadrons, or with $\geq 2\pi^0$ or η mesons, by $\pm 50(40)\%$.

Results for the corrected $\mathcal{B}$ values are shown in Table II. Adding the two mass regions, taking into account a partial cancellation of the missing fraction uncertainties in the ratio of $b \to d\gamma$ to $b \to s\gamma$, we find $\mathcal{B}(b \to d\gamma)/\mathcal{B}(b \to s\gamma) = 0.040 \pm 0.009(\text{stat}) \pm 0.010(\text{syst})$ in the mass range $M(X) < 2.0\ \text{GeV}/c^2$.

We correct for the unmeasured region $M(X) > 2.0\ \text{GeV}/c^2$ using the spectral shape from Kagan-Neubert [18] with the kinetic parameters $(m_b, \mu_\pi^2) = (4.65 \pm 0.05, -0.52 \pm 0.08)$ extracted from fits of $b \to s\gamma$ and $b \to c\ell\nu$ data [19], yielding corrections of 1.66 ± 0.03; the spectra for $b \to s\gamma$ and $b \to d\gamma$ are expected to be almost identical.

Conversion of the ratio of inclusive branching fractions to the ratio $|V_{td}/V_{ts}|$ is done according to [6], which requires the Wolfenstein parameters $\bar{\rho}$ and $\bar{\eta}$ as input. However, since the world average of these quantities relies on previous measurements of $|V_{td}/V_{ts}|$ we instead reexpress $\bar{\rho}$ and $\bar{\eta}$ in terms of $|V_{td}/V_{ts}|$ and the world average of the independent CKM angle β [15]. This procedure yields a value of $|V_{td}/V_{ts}| = 0.199 \pm 0.022(\text{stat}) \pm 0.024(\text{syst}) \pm 0.002(\text{th})$, compatible and competitive with more model-dependent determinations from the measurement of the exclusive modes $B \to (\rho, \omega)\gamma$ and $B \to K^*\gamma$ [2,3].

In summary, we have measured the inclusive $b \to s\gamma$ and $b \to d\gamma$ transition rates using a sum of seven final states in the hadronic mass range up to $2.0\ \text{GeV}/c^2$, making the first significant observation of the $b \to d\gamma$ transition in the region above $1.0\ \text{GeV}/c^2$. The value of $|V_{td}/V_{ts}|$ derived from these measurements has an experimental uncertainty approaching that from the measurement of exclusive decays $B \to (\rho, \omega)\gamma$ and $B \to K^*\gamma$, but a significantly smaller theoretical uncertainty.

We are grateful for the excellent luminosity and machine conditions provided by our PEP-II colleagues, and for the substantial dedicated effort from the computing organizations that support *BABAR*. The collaborating institutions wish to thank SLAC for its support and kind hospitality. This work is supported by DOE and NSF (USA), NSERC (Canada), CEA and CNRS-IN2P3 (France), BMBF and DFG (Germany), INFN (Italy), FOM (The Netherlands), NFR (Norway), MES (Russia), MICIIN (Spain), STFC (United Kingdom). Individuals have received support from the Marie Curie EIF (European Union), the A. P. Sloan Foundation (USA) and the Binational Science Foundation (USA-Israel).

[1] S. Bertolini, F. Borzumati, and A. Masiero, Nucl. Phys. **B294**, 321 (1987); H. Baer and M. Brhlik, Phys. Rev. D **55**, 3201 (1997); J. Hewett and J. Wells, Phys. Rev. D **55**, 5549 (1997); M. Carena *et al.*, Phys. Lett. B **499**, 141 (2001).

[2] D. Mohapatra *et al.* (Belle Collaboration), Phys. Rev. Lett. **96**, 221601 (2006).

[3] B. Aubert *et al.* (*BABAR* Collaboration), Phys. Rev. Lett. **98**, 151802 (2007).

[4] P. Ball, G. Jones, and R. Zwicky, Phys. Rev. D **75**, 054004 (2007).

[5] A. Abulencia *et al.* (CDF Collaboration), Phys. Rev. Lett. **97**, 242003 (2006).

[6] A. Ali, H. Asatrian, and C. Greub, Phys. Lett. B **429**, 87 (1998).

[7] B. Aubert *et al.* (*BABAR* Collaboration), Phys. Rev. Lett. **102**, 161803 (2009).

[8] B. Aubert *et al.* (*BABAR* Collaboration), Nucl. Instrum. Methods Phys. Res., Sect. A **479**, 1 (2002).

[9] G. C. Fox and S. Wolfram, Nucl. Phys. **B149**, 413 (1979).

[10] L-moments are defined as $L_i \equiv \sum_j p_j^* \cdot |\cos\theta_j^*|^i / \sum_j p_j^*$ and $\tilde{L}_i \equiv \sum_j p_j^* \cdot |\sin\theta_j^*|^i / \sum_j p_j^*$, where p_j^* and θ_j^* are the momentum and angle with respect to a given axis, respectively, for each particle j in the ROE.

[11] B. Aubert *et al.* (*BABAR* Collaboration), Phys. Rev. Lett. **89**, 201802 (2002).

[12] M. J. Oreglia, Ph.D. Thesis, Stanford University [SLAC Report No. 236, Appendix D, 1980 (unpublished)]; J. E. Gaiser, Ph.D. Thesis, Stanford University [SLAC Report No. 255, Appendix F, 1982 (unpublished)]; T. Skwarnicki, Ph.D. Thesis, Institute for Nuclear Physics, Krakow, Poland [DESY Report No. F31-86-02, Appendix E, 1986 (unpublished)].

[13] The Cruijff function is a centered Gaussian with different left-right resolutions and non-Gaussian tails: $f(x) = \exp((x-m)^2/(2\sigma_{L,R}^2 + \alpha_{L,R}(x-m)^2))$.

[14] H. Albrecht *et al.* (ARGUS Collaboration), Phys. Lett. B **185**, 218 (1987).

[15] E. Barberio *et al.* (Heavy Flavor Averaging Group), arXiv:0704.3575.

[16] T. Sjöstrand, arXiv:hep-ph/9508391; Comput. Phys. Commun. **82**, 74 (1994).

[17] B. Aubert *et al.* (*BABAR* Collaboration), Phys. Rev. D **72**, 052005 (2005).

[18] A. L. Kagan and M. Neubert, Phys. Rev. D **58**, 094012 (1998).

[19] O. Buchmüller and H. Flächer, Phys. Rev. D **73**, 073008 (2006).